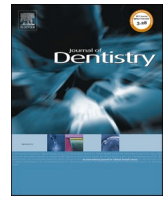




Since January 2020 Elsevier has created a COVID-19 resource centre with free information in English and Mandarin on the novel coronavirus COVID-19. The COVID-19 resource centre is hosted on Elsevier Connect, the company's public news and information website.

Elsevier hereby grants permission to make all its COVID-19-related research that is available on the COVID-19 resource centre - including this research content - immediately available in PubMed Central and other publicly funded repositories, such as the WHO COVID database with rights for unrestricted research re-use and analyses in any form or by any means with acknowledgement of the original source. These permissions are granted for free by Elsevier for as long as the COVID-19 resource centre remains active.



## Efficacy and hazards of 425 nm oral cavity light dosing to inactivate SARS-CoV-2

Max A. Stockslager<sup>\*</sup>, Jacob F. Kocher, Leslee Arwood, Nathan Stasko, Rebecca A. McDonald, Mark A. Tapsak, David Emerson

EmitBio Inc., 4222 Emperor Blvd, Suite 470, Durham, NC 27703, United States

### ARTICLE INFO

#### Keywords:

Light  
Photomedicine  
Hazard analysis  
COVID-19  
SARS-CoV-2  
Cytotoxicity

### ABSTRACT

**Objective:** Using a battery of preclinical tests to support development of a light-based treatment for COVID-19, establish a range of 425 nm light doses that are non-hazardous to the tissues of the oral cavity and assess whether a 425 nm light dose in this non-hazardous range can inactivate SARS-CoV-2 in artificial saliva.

**Methods:** The potential hazards to oral tissues associated with a range of acute 425 nm light doses were assessed using a battery of four preclinical tests: (1) cytotoxicity, using well-differentiated human large airway and buccal epithelial models; (2) toxicity to commensal oral bacteria, using a panel of model organisms; (3) light-induced histopathological changes, using *ex vivo* porcine esophageal tissue, and (4) thermal damage, by dosing the oropharynx of intact porcine head specimens. Then, 425 nm light doses established as non-hazardous using these tests were evaluated for their potential to inactivate SARS-CoV-2 in artificial saliva.

**Results:** A dose range was established at which 425 nm light is not cytotoxic in well-differentiated human large airway or buccal epithelial models, is not cytotoxic to a panel of commensal oral bacteria, does not induce histopathological damage in *ex vivo* porcine esophageal tissue, and does not induce thermal damage to the oropharynx of intact porcine head specimens. Using these tests, no hazards were observed for 425 nm light doses less than 63 J/cm<sup>2</sup> delivered at irradiance less than 200 mW/cm<sup>2</sup>. A non-hazardous 425 nm light dose in this range (30 J/cm<sup>2</sup> at 50 mW/cm<sup>2</sup>) was shown to inactivate SARS-CoV-2 *in vitro* in artificial saliva.

**Conclusion:** Preclinical hazard assessments and SARS-CoV-2 inactivation efficacy testing were combined to guide the development of a 425 nm light-based treatment for COVID-19.

**Clinical significance:** The process used here to evaluate the potential hazards associated with 425 nm acute light dosing of the oral cavity to treat COVID-19 can be extended to other wavelengths, anatomical targets, and therapeutic applications to accelerate the development of novel photomedicine treatments.

### 1. Introduction

Photomedicine refers to the use of light to induce photophysical and photochemical effects in the body for the treatment of disease. An early recorded use of photomedicine combined sunlight exposure with plant ingestion to treat vitiligo in 1400 BCE India [1]. Photomedicine achieved a significant milestone in 1903 when Niels Ryberg Finsen was awarded the Nobel Prize in Physiology or Medicine following successful treatment of Niemann-Pick's disease (1890), smallpox (1893), and lupus vulgaris (1895) with light, "in recognition of his contribution to the treatment of diseases [...] with concentrated light radiation, whereby he has opened a new avenue for medical science" [2]. Today, light-based therapies have been approved or cleared for several clinical

indications, including psoriasis, skin ulcers, and jaundice, and are under investigation for other indications including oral mucositis [3–5]. The most impactful applications of photomedicine to date have been for skin disorders, in part because light doses can be delivered to the skin conveniently and non-invasively.

As an extension to skin disorders, the oral cavity is an appealing target for photomedicine. Oral cavity light dosing is especially attractive as a candidate therapy for diseases caused by pathogens because the oral mucosal tissues act as a reservoir for pathogens and delivering light doses to these infected tissues could potentially mitigate the progression of such diseases. For example, it is well-known that ultraviolet (UV) light doses (<400 nm) are effective at inactivating viral pathogens such as SARS-CoV-2, the causative agent of coronavirus disease 2019 (COVID-

<sup>\*</sup> Corresponding author.

E-mail address: [mstockslager@emitbio.com](mailto:mstockslager@emitbio.com) (M.A. Stockslager).

<https://doi.org/10.1016/j.jdent.2022.104203>

Received 14 April 2022; Received in revised form 7 June 2022; Accepted 16 June 2022

Available online 17 June 2022

0300-5712/© 2022 The Authors. Published by Elsevier Ltd. This is an open access article under the CC BY-NC-ND license (<http://creativecommons.org/licenses/by-nc-nd/4.0/>).

19), on surfaces [6]. If UV light could be delivered safely to tissues infected with SARS-CoV-2 in the oral cavity, the treatment could directly reduce local viral burden, potentially allowing the host response to more rapidly resolve the infection [6]. However, UV light dosing of the oral cavity may be difficult to reduce to clinical utility since these wavelengths are also highly cytotoxic [7].

As an alternative to virus inactivation with cytotoxic UV wavelengths, delivering precisely-engineered doses of visible (>400 nm) light to the oral cavity has emerged as a promising approach for *in situ* SARS-CoV-2 inactivation. In particular, data from several groups suggests that 425 nm light doses inhibit the replication of SARS-CoV-2 in both cell lines (Vero E6) and in well-differentiated human large airway epithelial models (MatTek EpiAirway), and in a 31 subject, randomized, double-blind, sham-controlled early feasibility clinical trial it was observed that twice-daily dosing of the oropharynx and surrounding tissues with 16 J/cm<sup>2</sup> doses of 425 nm light reduced the mean time to COVID-19 symptom resolution by 57 h with a corresponding reduction in viral load in saliva [8–10]. Further, another clinical trial is ongoing whose objective is to confirm the results of the 31-subject trial in a larger population and for two different light doses (24 J/cm<sup>2</sup> and 32 J/cm<sup>2</sup>) [11].

In addition to evaluating the efficacy of acute light doses for SARS-CoV-2 inactivation and clinical benefit, it is critical to evaluate both hazards (*i.e.*, potential harms that could occur due to light dosing) and clinical safety (*i.e.*, that a particular clinical device does not present unacceptable risks). Previously, *in vitro* hazard assessments established that antiviral 425 nm light doses up to 60 J/cm<sup>2</sup> doses are not cytotoxic in cell lines (Vero E6) and that doses up to 32 J/cm<sup>2</sup> are not cytotoxic in well-differentiated human large airway epithelial cells [10]. Further, in the 16 J/cm<sup>2</sup> early feasibility trial, there were no application site reactions and no device-related serious adverse events reported [9,11,12]. Although these prior hazard assessments [10,13] and initial clinical safety analyses are necessary steps toward the development of acute oral cavity light-dosing devices, continuing to evaluate potential hazards (through preclinical studies) and clinical safety (through clinical trials) is necessary, particularly for the novel application of photomedicine in the oral cavity for which there is limited clinical precedent. For this reason, in this work we sought to perform a more systematic preclinical *in vitro* assessment of the various potential hazards that could result from delivering acute 425 nm light doses to the oral cavity. This process of searching for evidence of potential hazards through multiple complementary investigations is consistent with the process outlined in 21 C.F.R. § 860.7 (2022) for assessing the safety of medical devices.

For medical devices that make physical contact with the body, there exist standard, established processes for assessing the potential for various common biocompatibility hazards such as cytotoxicity, sensitization, irritation, toxicity, and carcinogenicity. Many of these tests are conducted using *in vitro* models and are defined in standards such as ISO 10993 [14]; however, delivering acute light doses to the oral cavity presents a different set of potential hazards for which no standard battery of hazard assessments has been certified. Toward the goal of establishing a range of non-hazardous 425 nm light doses, in this work a standard preclinical process was defined for estimating the potential hazards associated with delivering acute light doses to the oral cavity analogous to the routine battery of preclinical tests used to assess the biocompatibility of devices that make physical contact with the body. A battery of four standard tests was defined: (1) cytotoxicity, using well-differentiated human large airway and buccal epithelial models; (2) toxicity to commensal oral bacteria, using an *in vitro* panel of model organisms; (3) light-induced histopathological changes, using *ex vivo* porcine esophagus tissue; and (4) thermal damage, by delivering light doses to the oropharynx of intact porcine head specimens. The proposed preclinical tests are based on *in vitro* and *ex vivo* models, in accordance with the preference described in ISO 10993 for minimizing the use of *in vivo* animal testing when “equally relevant information” can be obtained from alternative models [14]. The studies were designed to test the null

hypothesis that 425 nm light doses do not induce increased damage to the host tissues (either cytotoxicity, or histopathological damage, or thermal damage, depending on the test) or increased toxicity to commensal organisms compared to untreated controls. More broadly, these hazard assessments are intended to provide additional evidence that oral cavity light dosing can be non-hazardous and effective for SARS-CoV-2 inactivation, which should be presumed false until sufficient evidence is accumulated.

This process is applied to establish a range of non-hazardous 425 nm doses (defined as the total energy delivered per unit area at a particular wavelength) and irradiances (the rate at which light energy is delivered per unit time and area at a particular wavelength). In turn, it is shown that a 425 nm light dose established as non-hazardous using this process inactivates SARS-CoV-2 *in vitro* in artificial saliva. Finally, these results are presented in the context of existing FDA-cleared oral cavity light dosing devices as well as ongoing work using acute 425 nm light dosing of through the oral cavity to treat COVID-19 [9].

## 2. Methods

Custom assays were defined to assess four potential hazards that could result from dosing the oral cavity with light: (1) cytotoxicity, using well-differentiated human large airway and buccal epithelial models; (2) toxicity to commensal oral bacteria, using an *in vitro* panel of model organisms; (3) light-induced histopathological changes, using *ex vivo* porcine esophagus tissue; and (4) thermal damage, by delivering light doses to the oropharynx of intact porcine head specimens. In addition, a custom assay was developed to assess the potential of doses of 425 nm visible light to inactivate SARS-CoV-2 in artificial saliva. The range of doses and irradiances that can be tested is constrained by different practical limitations for each assay (*e.g.*, geometry of the test apparatus) or other effects that are an artifact of the model system and would not occur *in vivo* (*e.g.*, heating or evaporation of culture medium). Within the bounds of these limitations, the four assays were individually optimized to maximize internal consistency and repeatability and provide a useful framework for preclinical hazard assessment. Statistical analyses were performed using R (R Core Team; Vienna, Austria).

### 2.1. Cytotoxicity in well-differentiated human large airway and buccal epithelial models (AIR-100, ORL-200)

Primary models derived from well-differentiated human large airway epithelial cells (AIR-100; MatTek Corporation, Ashland, MA, USA) or well-differentiated human buccal epithelial cells (ORL-200; MatTek Corporation, Ashland, MA, USA) were acquired, revived, and stored as previously described [10]. Light dosing was performed with custom biological light units (BLUs; EmitBio, Inc., Durham, NC, USA), a platform optimized for repeatable light dosing of *in vitro* biological samples at the wavelength, irradiance, and duration of interest under temperature-controlled conditions [10]. Briefly, tissues were placed in 6-well plates (Costar 3506; Corning Inc., Corning, NY, USA) at room temperature and dosed with 405 and 425 nm light at an irradiance of 50 mW/cm<sup>2</sup>, resulting in doses ranging from 0 J/cm<sup>2</sup> (no exposure) to 256 J/cm<sup>2</sup> (85 min). A dose of 385 nm light at an irradiance of 25 mW/cm<sup>2</sup> for 80 min (resulting in a dose of 120 J/cm<sup>2</sup>) was used in AIR-100 as a positive control for cytotoxicity. Three-minute exposure to 3% hydrogen peroxide (Thermo Scientific 426,001,000; Thermo Fisher Scientific, Waltham, MA, USA), a GHS class III (mild) irritant routinely used in dental care, was used in ORL-200 as a positive control for cytotoxicity. The BLUs delivered light doses with <1% ultraviolet A (UVA; for the 425 nm source), 6% UVA (for the 405 nm source), and 92% UVA (for the 385 nm source). After light dosing, the tissues were incubated at 37 °C and 5% CO<sub>2</sub> for 3 h, then the cytotoxicity resulting from each light dose was evaluated using the MTT-100 assay (MTT-100; MatTek Corporation, Ashland, MA, USA) following the manufacturer’s instructions as previously described [15]. AIR-100 tissues were incubated with 3-(4,

5-dimethylthiazol-2-yl)-2,5-diphenyltetrazolium bromide (MTT) reagent for 90 min, while ORL-200 tissues were incubated with MTT reagent for 3 h. Tissue viability measured using the MTT assay was compared to threshold of 75% viability, which was previously validated in the AIR-100 model to determine the GHS Acute Inhalation Toxicity Category 1 and 2 and EPA Acute Inhalation Toxicity Category I-II classification [16]. Tissue viability was calculated relative to dark controls, and viability for each test condition was evaluated as the average of five biological replicates, providing sufficient power to detect a two-standard-deviation reduction in viability with 80% power and 95% confidence using a one-sided, two-sample *t*-test [17].

## 2.2. Microbicidal effects on commensal oral bacteria

Bacterial strains (names, vendors, and catalog numbers given in Table 1) were stored at  $-70^{\circ}\text{C}$  in medium containing 20% glycerol (Thermo Scientific J62399-AP; Thermo Fisher Scientific, Waltham, MA, USA), then cultured at  $37^{\circ}\text{C}$  on Mueller-Hinton agar (Difco 225250; Becton Dickinson, East Rutherford, NJ, USA) or shaking at 150 RPM in cation-adjusted Mueller-Hinton broth (Difco 225250; Becton Dickinson, East Rutherford, NJ, USA). All work was conducted under biosafety level-2 (BSL-2) guidelines. First, light dose responses over the range  $0\text{--}192\text{ J/cm}^2$  were measured for *Streptococcus mitis* (a Gram-positive commensal from most abundant genus in the oral microbiome [18]) and *Acinetobacter junii* (a Gram-negative member of Moraxellaceae, a family that contains several oral commensal species [19]). For light dose response measurements, bacterial strains were suspended in 1 mL phosphate-buffered saline (PBS; Gibco 10010023; Thermo Fisher Scientific, Waltham, MA, USA), then the bacterial density of each suspension was determined by  $\text{OD}_{600}$  and titrated to  $10^8$  colony forming units (CFU)/mL in phosphate-buffered saline. Bacterial suspensions were further diluted to  $1 \times 10^6$  CFU/mL in brain heart infusion broth (Difco 211059; Becton Dickinson, East Rutherford, NJ, USA). Two hundred  $\mu\text{L}$  of each bacterial culture was loaded into 96-well plates (25381-056; VWR, Radnor, PA, USA) for light dosing. Doses of 425 nm light were administered by a BLU at an irradiance of  $50\text{ mW/cm}^2$ , resulting in total light doses ranging from  $0\text{ J/cm}^2$  (no exposure) to  $192\text{ J/cm}^2$  (64 min). After light dosing, bacterial cultures were serially diluted in PBS then incubated for 18–24 h for enumeration of bacterial colonies after plating on species-specific agar plates (*Streptococcus* were grown on chocolate agar [E14; Hardy Diagnostics, Santa Maria, CA, USA]; *Acinetobacter junii*, *Arthrobacter albus*, *Gemella morbillorum*, *Rothia aeria*, and *Klebsiella* species were grown on BHI agar [Difco 241830; Becton Dickinson, East Rutherford, NJ, USA]; *Moraxella osloensis* was grown on nutrient agar [Difco 213000; Becton Dickinson, East Rutherford, NJ, USA];

**Table 1**  
Panel of representative commensal oral bacteria used for microbicidal hazard assessments.

Family	Species	Source and catalog number	Gram stain
Streptococcaceae	<i>Streptococcus mitis</i>	BEI; HM-262	Positive
Streptococcaceae	<i>Streptococcus sanguinis</i>	BEI; HM-275	Positive
Streptococcaceae	<i>Streptococcus intermedius</i>	BEI; HM-368	Positive
Micrococcaceae	<i>Arthrobacter albus</i>	BEI; HM-1152	Positive
Micrococcaceae	<i>Rothia aeria</i>	BEI; HM-818	Positive
Sporolactobacillaceae	<i>Gemella morbillorum</i>	ATCC 27,924	Positive
Actinomycetaceae	<i>Actinomyces viscosus</i>	ATCC 43,146	Positive
Moraxellaceae	<i>Moraxella osloensis</i>	ATCC 19,965	Negative
Enterobacteriaceae	<i>Klebsiella ozaenae</i> #51	AR-bank; 0051	Negative
Enterobacteriaceae	<i>Klebsiella ozaenae</i> #96	AR-bank; 0096	Negative
Enterobacteriaceae	<i>Klebsiella oxytoca</i> #28	AR-bank; 0028	Negative
Moraxellaceae	<i>Acinetobacter junii</i>	ATCC 17,908	Negative

*Actinomyces viscosus* was grown on Brucella blood agar plates [Difco 297716; Becton Dickinson, East Rutherford, NJ, USA]). The bactericidal threshold in these experiments was defined as a  $3\text{-log}_{10}$  (1000-fold) reduction in bacterial (quantified as CFU/mL) post-exposure. All samples were evaluated with biological duplicates and technical triplicates to provide sufficient power to detect a two-standard-deviation reduction in growth with 80% power and 95% confidence using a one-sided, two-sample *t*-test while also providing a second biological replicate for quality control purposes [17].

Next, bactericidal effects were evaluated at a single light dose ( $32\text{ J/cm}^2$ ) against a panel of twelve commensal bacteria strains found in the oral cavity (Table 1). The strains were selected for analysis based on their relative abundance in the oral cavity and their disproportionately higher prevalence in healthy microbiomes compared to periodontitis microbiomes [20]. Each species was evaluated using the same process described for the light dose response measurements, but at a single dose. Measurements were carried out in biological duplicates and technical triplicates, as described above.

Finally, longer-term effects of light dosing on bacterial growth were assessed in a subset of three species from the panel: *Streptococcus intermedius*, *Rothia aeria*, and *Klebsiella ozaenae* #51. Doses of 425 nm light were administered by a BLU at an irradiance of  $50\text{ mW/cm}^2$ , resulting in total light doses ranging from  $0\text{ J/cm}^2$  (no exposure) to  $32\text{ J/cm}^2$  (10.7 min). After light dosing was performed using the same process described previously, bacteria were incubated for 24 h at  $37^{\circ}\text{C}$  stationary (*S. intermedius*) or with shaking (*R. aeria* and *K. ozaenae* #51), then enumerated after 24 h using the same process described previously, again in biological duplicates and technical triplicates.

## 2.3. Light-induced histopathological damage in ex vivo porcine esophageal tissue

The potential for light dosing of the oral cavity to cause histopathological damage in and around tissues of the oral cavity was assessed using *ex vivo* porcine esophageal tissue. This model system was chosen because porcine epithelial tissues are accepted models for human epithelial tissue due to their anatomical similarity, particularly compared to other species such as rat [21,22]. Porcine oral tissue was not used since the surface area is insufficient for conducting multiple dosing experiments. Esophagus tissue from a recently-euthanized Yucatan miniature pig was used for *ex vivo* experiments. All measurements were completed within 2 h of euthanasia. After gross necropsy, the esophagus was cut lengthwise using a #10 scalpel (MyMed SLT-03/SC#10; Amazon, Seattle, WA) to form a rectangle of tissue, and then sectioned into discrete test specimen portions (measuring approximately  $5\text{ mm} \times 30\text{ mm}$ ) for each condition. Three biological replicates were used for each of five test conditions. Sample sizes were determined by practical limitations rather than *ex ante* power calculations; given that a maximum of approximately 15 tissue pieces could be cut from one esophagus, our study design represented the maximum number of biological replicate measurements that could be performed for each of the five conditions of interest. The samples were placed on a pre-warmed,  $8'' \times 8''$  anodized 6061 aluminum plate (9246K31; McMaster-Carr, Elmhurst, IL, USA), which was heated by a hot plate (Waverly HS2-S; SoCal BioMed, Lake Forest, CA, USA) set to  $37^{\circ}\text{C} \pm 3^{\circ}\text{C}$  to maintain a consistent thermal boundary condition. Light doses were delivered using BLUs, then specimens were fixed in 10% neutral buffered formalin (Fisher Scientific SF100-4; Thermo Fisher Scientific, Waltham, MA, USA) for 96 h, sectioned (8 transverse sections taken  $0.75\text{ mm}$  apart), then mounted and stained with hematoxylin and eosin (H&E) by Scientific Solutions, LLC (Fridley, MN) using routine paraffin histology techniques. Slides were evaluated for markers of thermal or histopathological damage by a board-certified pathologist who was blinded to the study conditions.

#### 2.4. Thermal hazards in the oropharynx in intact ex vivo porcine head specimens

To assess the potential for acute light doses to cause excessive heating of the tissues in the oral cavity, the oropharynx of the intact porcine head was considered a suitable model due to its anatomical similarity to the same anatomy in humans. Specifically, the oropharynx of an intact porcine head specimen was exposed to acute light doses, then the resulting temperature increases were measured and compared to allowable maximum temperature increases previously described in the thermal hazard literature for similar tissues.

A porcine head specimen was obtained from local market sources and stored at 4 °C until use. A glossectomy was performed, with the tissue surrounding the oropharynx left intact to ensure that this experimental model is representative of extended musculoskeletal structures surrounding the oropharynx *in vivo*. One animal replicate was used in this study, with three replicate treatments used for each dose level. One animal replicate with multiple replicate treatments was considered a suitable study design because the ultimate goal is to deliver light doses to the human oral cavity, and differences between the oral cavities of different pigs appear to be small compared to the differences between the porcine and human oral cavities.

To monitor the transient increase in tissue temperature that resulted from an acute light dose, a K-type thermocouple probe (TL0260; PerfectPrime, London, England) was inserted into the tissue and monitored using a data logger thermometer (TC0520; PerfectPrime, London, England). The target thermocouple location was the center of the dosed area because this is the point at which the tissue temperature increases most. To position the thermocouple probe in the tissue, an 18-gage needle (305195; Becton Dickinson, East Rutherford, NJ, USA) was positioned at the desired thermocouple position, the thermocouple was threaded through the needle, the needle was removed, and then the thermocouple was secured with thread (8800K41; McMaster-Carr, Elmhurst, IL, USA) to prevent it from retreating into the tissue. The thermocouple tip was positioned just below the surface of the oropharynx without protruding into the oral cavity.

Light doses were delivered using a custom light dosing device consisting of 425 nm LEDs (L1C1-VLT10000CACM0; Lumileds, Amsterdam, Netherlands), driver (LM3410XSD/NOPB; Texas Instruments, Dallas, TX, USA), lens (ACL25416U; Thorlabs, Newton, NJ, USA), and a programmable power supply (BK Precision 9201; DigiKey, Thief River Falls, MN, USA). Before each measurement, the lens of the light dosing device was positioned at a pre-specified distance from the oropharynx (either 67 mm or 40 mm) using an adjustable ring stand system (50165A33, 50165A64, 50165A69, 50165A13; McMaster-Carr, Elmhurst, IL, USA). The light dose was delivered over 20 min while the tissue temperature and ambient temperature were recorded. After each measurement, the tissue was allowed to cool to room temperature (20 °C ± 1 °C) before repeating. Three replicate measurements were performed at each of four different irradiances: 415 mW/cm<sup>2</sup> (total dose 498 J/cm<sup>2</sup> over 20 min); 266 mW/cm<sup>2</sup> (total dose 319 J/cm<sup>2</sup> over 20 min); 210 mW/cm<sup>2</sup> (total dose 252 J/cm<sup>2</sup> over 20 min); and 147 mW/cm<sup>2</sup> (total dose 176 J/cm<sup>2</sup> over 20 min); data from one replicate (at 266 mW/cm<sup>2</sup>) was excluded due to a temperature logger error. The cumulative equivalent minutes at 43 °C (CEM<sub>43</sub>) statistic was used to assess the cumulative thermal damage resulting from the transient light-induced temperature increase. The CEM<sub>43</sub> statistic is intended to equate a thermal transient across a range of temperatures into an equivalent amount of time at 43 °C that would cause a similar level of thermal damage [23]. The value of 43 °C was selected based on studies that observed little cell death at lower temperatures but rapidly increasing cell death at higher temperatures; above this temperature, every additional 1 °C change increases the incremental rate of thermal damage by approximately a factor of two [24, 25]. Depending on the tissue, typical maximum allowable CEM<sub>43</sub> values are on the order of 1–10 min [24]. Beyond this thermal dose, irreversible thermal damage such as necrosis can occur. The CEM<sub>43</sub> statistic is

defined as the exponentially-weighted deviation of the tissue temperature from 43 °C integrated over the treatment duration, *i.e.*,

$$CEM_{43} = \sum_i R_i^{(43^\circ\text{C}-T_i)} \Delta t \quad (1)$$

where *i* indexes the discrete temperature measurements, *T<sub>i</sub>* is the temperature at time *t<sub>i</sub>*,  $\Delta t$  is the (constant) time between discrete temperature measurements, and *R<sub>i</sub>* is a dimensionless constant equal to 0.25 when *T<sub>i</sub>* < 43 °C and 0.50 when *T<sub>i</sub>* ≥ 43 °C [26]. Measurements were performed with the tissue starting at ambient room temperature. To compute the CEM<sub>43</sub> statistic, we measured the temperature increase resulting from light treatment and added this to physiological temperature (37 °C) to estimate the temperatures that would be reached if the light doses were instead delivered *in vivo*.

#### 2.5. Inactivation of SARS-CoV-2 in artificial saliva by acute 425 nm light doses

To assess the potential of doses of 425 nm light to inactivate SARS-CoV-2 in artificial saliva, cell-free inactivation assays were conducted with virus diluted in a panel of artificial salivas. The inactivation studies were conducted as previously described [10], but with virus light dosing performed in artificial salivas or in culture medium (Minimal Essential Medium [Gibco 11095-080; Thermo Fisher Scientific, Waltham, MA, USA] supplemented with 2% fetal bovine serum [Gibco 10082-147; Thermo Fisher Scientific, Waltham, MA, USA], 1% non-essential amino acids [Gibco 11140076; Thermo Fisher Scientific, Waltham, MA, USA], and 1% antibiotic-antimycotic [Gibco 15240-062; Thermo Fisher Scientific, Waltham, MA, USA]). Artificial salivas used in dental alloy research (BZ108), oral pharmaceutical delivery (BZ109), and medical and dental research (BZ184) were obtained (BZ108, BZ109, and BZ184; Biochemazone, Edmonton, Canada). SARS-CoV-2 WA1 (BEI Resources; BEI Resources, Manassas, VA, USA) was diluted in each artificial saliva to a final concentration of 2 × 10<sup>6</sup> plaque-forming units/milliliter (PFU/mL). SARS-CoV-2 WA1 and Vero E6 cells (VERO C1008; ATCC, Manassas, VA, USA) were propagated as previously described [10]. Briefly, diluted virus (500 μL) was exposed to the indicated doses of 425 nm light using BLUs, then viral titers were enumerated after exposure using a plaque assay. Four biological replicates were assessed per condition, providing sufficient power to detect a two-standard-deviation reduction in mean viral titer with 80% power and 95% confidence using an unpaired, two-sample, one-sided *t*-test [17]. All work with replication-competent virus was conducted under biosafety level-3 (BSL-3) conditions following strict adherence to established biosafety guidelines.

### 3. Results

#### 3.1. Cytotoxicity in well-differentiated human large airway and buccal epithelial models (AIR-100, ORL-200)

AIR-100 tissue viability was greater than 75% for 425 nm light doses of 7.5, 15, 30, 60, 120, and 160 J/cm<sup>2</sup> and for 405 nm light doses of 7.5, 15, 30 and 60 J/cm<sup>2</sup> (Fig. 1A). AIR-100 viability was reduced to 2% of control tissues following a 385 nm light dose of 120 J/cm<sup>2</sup>. Greater than 100% viability relative to controls was observed in AIR-100 for 425 nm light doses of 7.5 and 15 J/cm<sup>2</sup>, and for 405 nm light doses of 7.5, 15, 30 and 60 J/cm<sup>2</sup>.

ORL-200 tissue viability was greater than 75% for 425 nm light doses of 0, 7.5, 15, 30, 60 and 120 J/cm<sup>2</sup> (Fig. 1B). ORL-200 viability was reduced to 2.6% following three minutes exposure to 3% hydrogen peroxide (H<sub>2</sub>O<sub>2</sub>).

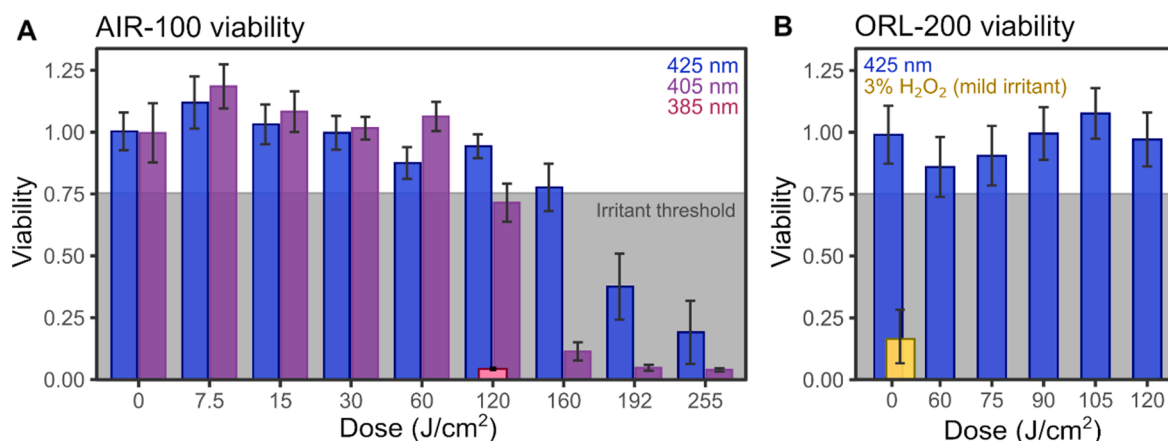


**Fig. 1.** Assessment of acute light dose-induced cytotoxicity in well-differentiated human large airway or oral epithelial models. (A) AIR-100 (the MatTek EpiAirway model) was dosed with 405 nm and 425 nm light at doses up to 255 J/cm<sup>2</sup>. As a positive control, a 120 J/cm<sup>2</sup> dose of UV (385 nm) light reduced viability to 4.3%. (B) ORL-200 (the MatTek EpiOral model) was dosed with 425 nm light at doses of up to 120 J/cm<sup>2</sup>. As a positive control, three minutes exposure to 3% hydrogen peroxide (H<sub>2</sub>O<sub>2</sub>), a known mild irritant, reduced ORL-200 viability to 2.6% ( $n = 5$  replicates per dose; error bars represent standard deviation).

### 3.2. Microbicidal effects on commensal oral bacteria

The Gram-positive organism *Streptococcus mitis* showed no reduction in viability across the full range of 425 nm light doses of 32, 64, 96, 128, 160, and 192 J/cm<sup>2</sup> (Fig. 2A). The Gram-negative organism *A. junii* showed no reduction in viability at a 425 nm light dose of 32 J/cm<sup>2</sup>, but a dose-dependent decrease in viability was observed at doses of 64 J/cm<sup>2</sup> and higher (Fig. 2B), with >3 log<sub>10</sub> reduction observed at doses of 96, 128, 160, and 192 J/cm<sup>2</sup>.

Next, a 32 J/cm<sup>2</sup> dose of 425 nm light was delivered to the panel of 12 commensal microbes (Table 1) and compared to dark controls after a 24 h recovery period (Fig. 3A, B). Light-induced changes in bacterial counts ranged from -0.4 log<sub>10</sub> to +0.1 log<sub>10</sub> compared to dark controls. To ensure that the acute light doses did not arrest bacterial growth beyond 24 h, in an independent experiment the growth of three of the commensals (*S. intermedius*, *R. aeria*, and *K. ozaenae* #51) was followed for an additional 24 h after light dosing. Growth was still observed during this period (Supplemental Fig. 1).

### 3.3. Light-induced histopathological damage in ex vivo porcine esophageal tissue

A variety of histopathological changes were observed in the porcine

esophageal tissue specimens following *ex vivo* light dosing (Fig. 4; Supplemental Fig. 2). Compared to non-dosed tissues (Fig. 4A), tissues exposed to the maximum light dose (204 J/cm<sup>2</sup>) exhibited a variety of changes indicative of thermal damage, including coagulative changes in the lamina propria; vacuolar change, cell separation, and nuclear shrinkage in the tunica muscularis; basal cell vacuolization and clefting; and nuclear streaming (Fig. 4B). In tissues receiving 0 J/cm<sup>2</sup>, 30 J/cm<sup>2</sup>, and 60 J/cm<sup>2</sup> light doses, there were no proprial changes (Fig. 4C), basal vacuolization or clefting (Fig. 4D), no smooth muscle changes (Fig. 4E), and only mild nuclear streaming (21% of sections; Fig. 4F). Moderate changes in the four markers were observed in tissues exposed to 120 J/cm<sup>2</sup> light doses, and the greatest changes were observed in tissues exposed to 204 J/cm<sup>2</sup> light doses. The observed variability between replicates for the various pathological features appears to be an artifact of the sample preparation process, during which tissue specimens were manually dissected from an intact porcine esophagus, resulting in some variability in the size and shape of the tissue specimens; however, the observed variability between biological replicates does not change the trend of significant damage at a dose of 120 and 204 J/cm<sup>2</sup> and minimal damage at doses of ≤60 J/cm<sup>2</sup>.

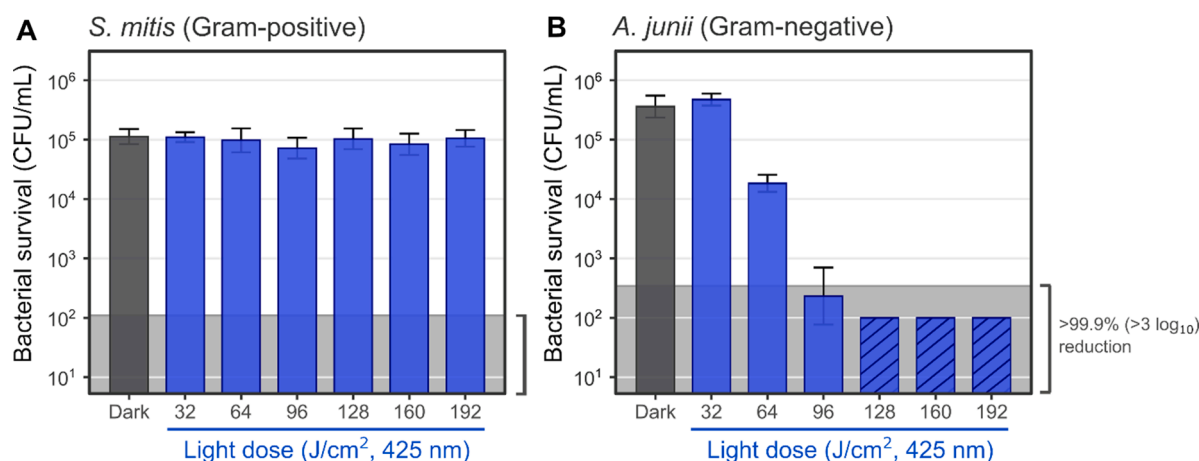


**Fig. 2.** Acute light dose responses of two representative commensal microbes. (A) Acute 425 nm light doses of 32, 64, 96, 128, 160, or 192 J/cm<sup>2</sup> did not reduce the growth of *S. mitis*, a Gram-positive commensal microbe. (B) Acute 425 nm light doses of 32 J/cm<sup>2</sup> did not reduce the growth of *A. junii*, a Gram-negative commensal microbe, but a dose-dependent reduction in growth was observed at doses of 64 J/cm<sup>2</sup> and higher. Data plotted as geometric mean  $\pm$  standard deviation;  $n = 6$  replicates per condition.

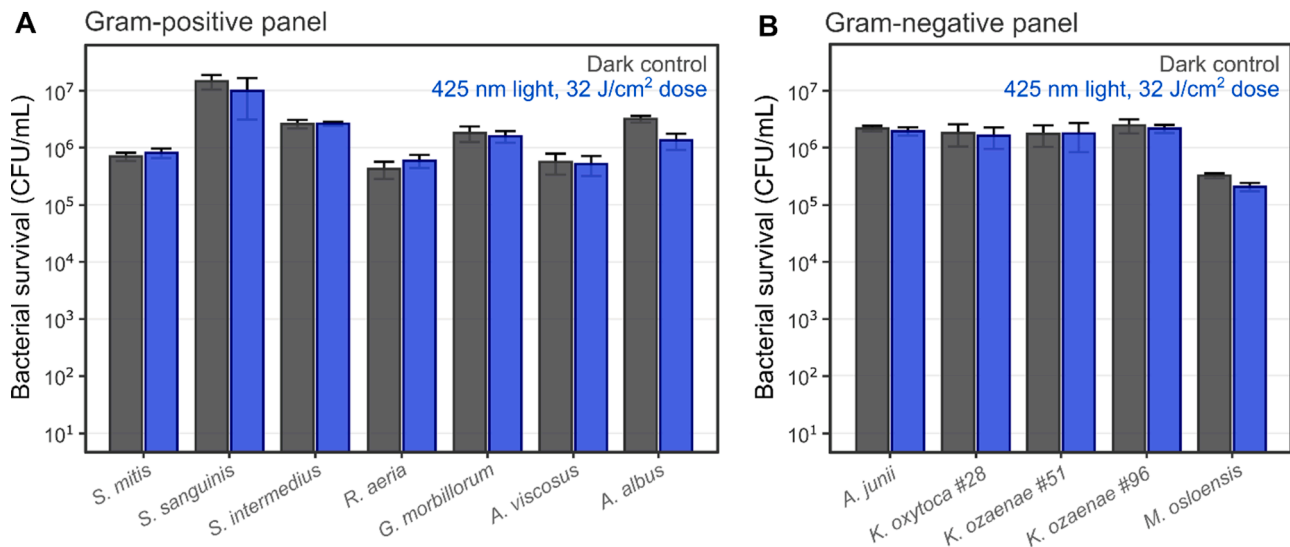


**Fig. 3.** Assessment of microbicidal hazards of acute light dosing using a panel of commensal oral bacteria. An acute 425 nm light dose of 32 J/cm<sup>2</sup> was not bactericidal to any of a panel of 12 commensal microbes, of which 7 were Gram-positive (A) and 5 were Gram-negative (B). Data plotted as geometric mean  $\pm$  standard deviation;  $n = 6$  replicates per condition.

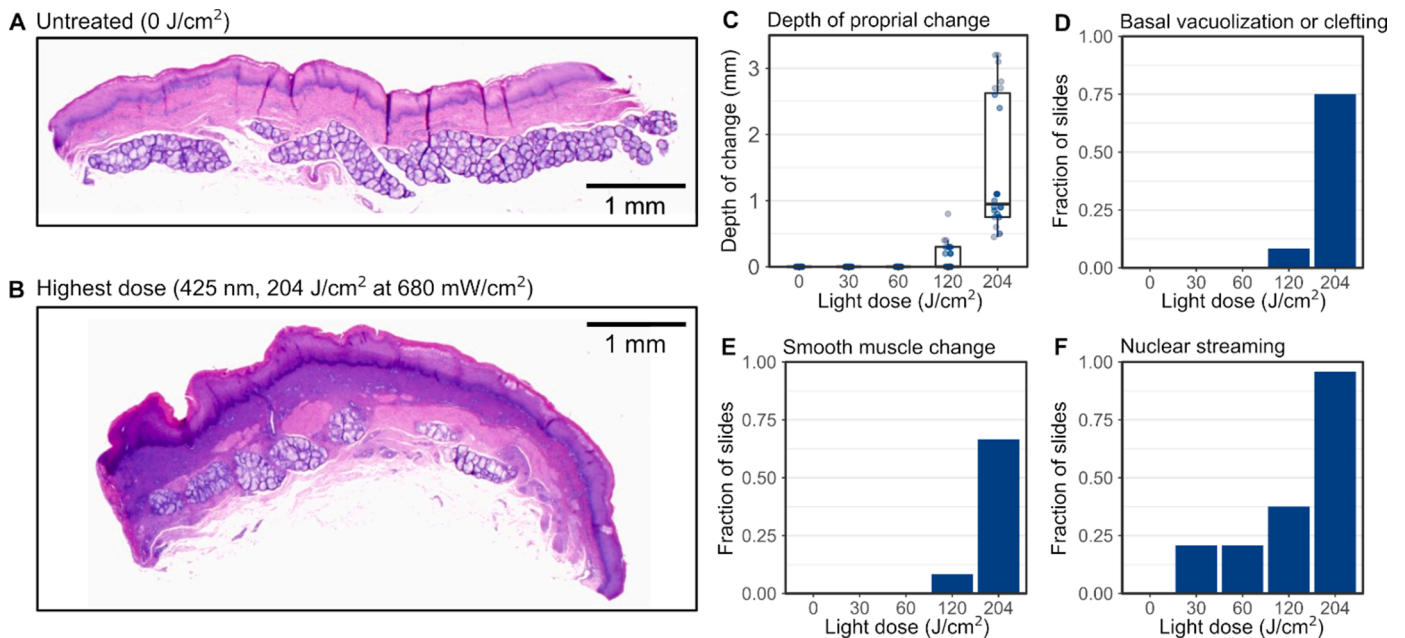


**Fig. 4.** Histopathological damage in response to acute light doses in porcine esophageal tissue. (A-B) Esophageal tissue specimens exposed to acute doses of 425 nm light exhibited a variety of pathological changes characteristic of thermal damage (as observed with H&E staining), including: (C) damage to the lamina propria, in particular a zone of increased hematoxylin staining, consistent with leakage of nuclear contents from cells to the surrounding matrix; (D) basal cell vacuolization and clefting; (E) changes in the smooth muscle layer; and (F) nuclear streaming (or “string-bean” nuclei), a characteristic marker of thermal injury previously described in the literature. Only mild changes were observed at light doses less than 120 J/cm<sup>2</sup>.

### 3.4. Thermal hazards in the oropharynx of intact porcine head specimens

In the intact porcine head specimen (Fig. 5A), over the 20-min dosing duration, tissue temperature increased from ambient by a maximum of 3.5 °C  $\pm$  0.5 °C (at 147 mW/cm<sup>2</sup>), 8.4 °C  $\pm$  0.6 °C (at 210 mW/cm<sup>2</sup>), 14 °C  $\pm$  1 °C (at 266 mW/cm<sup>2</sup>), and 19.5 °C  $\pm$  0.9 °C (at 415 mW/cm<sup>2</sup>) (Fig. 5B). CEM<sub>43</sub> statistics were >20 min (at 147 mW/cm<sup>2</sup>), 13  $\pm$  1 min (at 210 mW/cm<sup>2</sup>), 6.0  $\pm$  0.5 min (at 266 mW/cm<sup>2</sup>), and 3.8  $\pm$  0.1 min (at 415 mW/cm<sup>2</sup>) (Fig. 5C). The light doses that resulted in 1 min CEM<sub>43</sub> were >176 J/cm<sup>2</sup> (>20 min at 147 mW/cm<sup>2</sup>), 91  $\pm$  7 J/cm<sup>2</sup> (7.2  $\pm$  0.6 min at 210 mW/cm<sup>2</sup>), 54  $\pm$  5 J/cm<sup>2</sup> (3.4  $\pm$  0.3 min at 266 mW/cm<sup>2</sup>), and 58  $\pm$  3 J/cm<sup>2</sup> (2.3  $\pm$  0.1 min at 415 mW/cm<sup>2</sup>).

### 3.5. Inactivation of SARS-CoV-2 in artificial saliva by acute 425nm light doses

Dose-dependent reductions in SARS-CoV-2 titer were observed for virus diluted in cell culture medium and in the three artificial saliva matrices tested (Fig. 6). In all three artificial salivas, SARS-CoV-2 titer was reduced by >1 log<sub>10</sub> at 7.5 J/cm<sup>2</sup> and >3 log<sub>10</sub> (below the assay detection limit) at 30 J/cm<sup>2</sup> and 60 J/cm<sup>2</sup> (Fig. 6). In this experiment, the reduction in SARS-CoV-2 titer observed in the artificial salivas was greater than the reduction observed for virus diluted in culture medium, where SARS-CoV-2 titer was reduced by 0.9 log<sub>10</sub> at 7.5 J/cm<sup>2</sup>, >2 log<sub>10</sub> at 30 J/cm<sup>2</sup>, and >3 log<sub>10</sub> (below the assay detection limit) at 60 J/cm<sup>2</sup>.

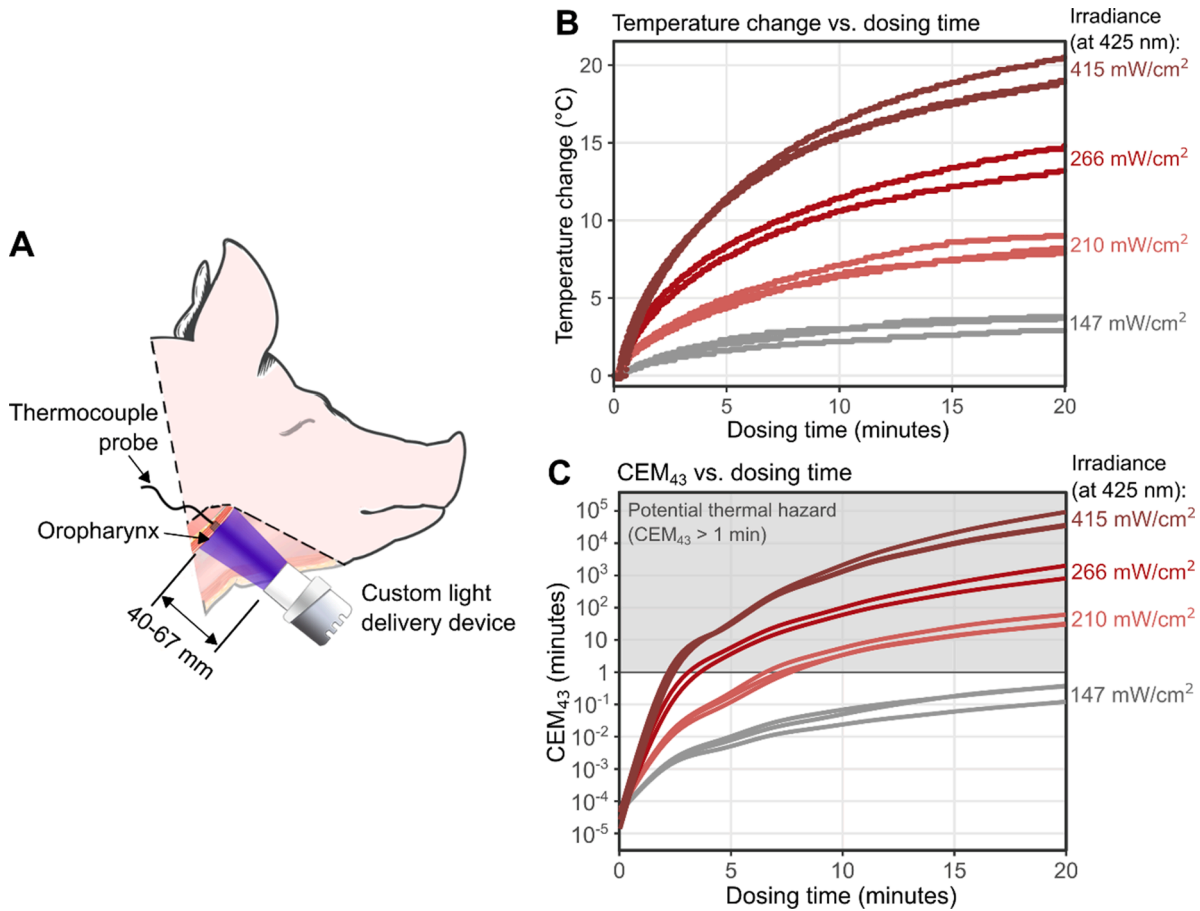


Fig. 5. Assessment of thermal hazards of acute light dosing to the oropharynx of an intact porcine head. (A) Schematic of the thermal hazard testing approach. Light doses were delivered to the oropharynx of an intact porcine head. (B) Temperature increases (from ambient) recorded during light dosing of the oropharynx of an intact porcine head specimen with 425 nm light at irradiances ranging from 147 to 415 mW/cm<sup>2</sup> for 20 min (with total doses over 20 min ranging from 176 to 498 J/cm<sup>2</sup>). (C) CEM<sub>43</sub> statistics were calculated based on these temperature profiles and compared to a thermal hazard threshold of 10 min CEM<sub>43</sub>.

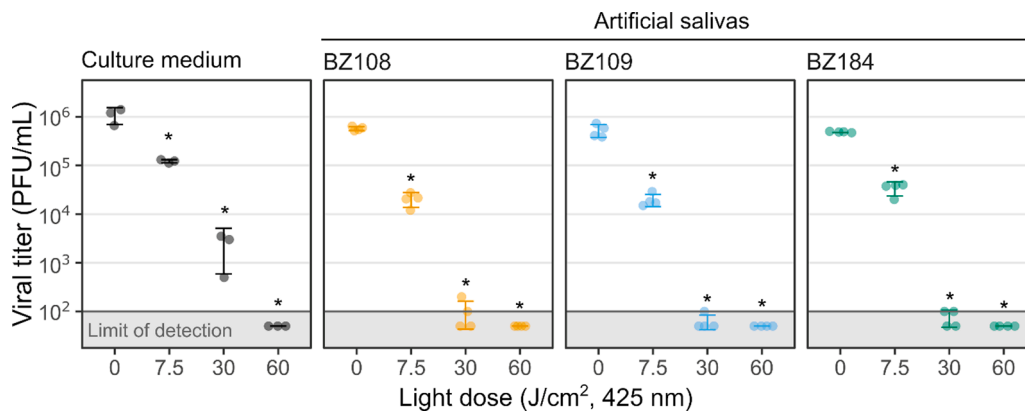


Fig. 6. Inactivation of SARS-CoV-2 in artificial saliva by 425 nm light doses. In culture medium and artificial saliva (BZ108, BZ109, or BZ184), SARS-CoV-2 titer is significantly reduced by 425 nm light doses of 7.5 J/cm<sup>2</sup> or greater, and is reduced by >3 log<sub>10</sub> (below the assay detection limit) at 60 J/cm<sup>2</sup>. Viral titers are reported in mean plaque-forming units (PFU) per mL ± standard deviation. \*p < 0.01, unpaired t-test.

#### 4. Discussion

It is well known that doses of light, especially UV light, can inactivate viruses that cause respiratory illness; however, reduction of a light-based treatment to clinical utility has been limited by the potential hazards and associated safety risks introduced by delivering doses of light that contain enough energy to inactivate virus. In this study, we sought to determine whether a dose of 425 nm visible light established

as non-hazardous to oral tissue in a battery of pre-clinical hazard assessment tests can inactivate SARS-CoV-2 in artificial saliva and serve as the basis for the light-based treatment of COVID-19. The null hypothesis tested by each hazard assessment was that 425 nm light doses do not induce increased damage to the host tissues (either cytotoxicity, or histopathological damage, or thermal damage, depending on the test) or increased toxicity to commensal organisms compared to untreated controls.

The first hazard assessed was the potential for acute light doses to induce cytotoxicity in target tissues of the oral cavity. Because there has been limited study in large airway or oral models of light-induced cytotoxicity, established procedures for assessing cytotoxicity in response to chemical irritants were used as a baseline [16]. Well-differentiated human large airway and buccal tissue models such as EpiAirway (MatTek AIR-100) and EpiOral (ORL-200, MatTek) have been used previously for assessing the effects of chemical irritants, and because these models do not exhibit any obvious characteristics that suggest they would respond differently to light than other cell types of the oral cavity, we considered them well-suited for assessing light-induced cytotoxicity as well. In the chemical irritant literature, reduction of viability below 75% of untreated AIR-100 models has been previously validated as a marker for airway irritation [16]. Although this threshold was determined using AIR-100, it was considered suitable to apply as a threshold for irritation in ORL-200 as well due to the structural similarity between the two models (*i.e.*, both are 5–10 cell layers thick and are derived from well-differentiated normal human epithelial cells). Both positive cytotoxicity controls (3% hydrogen peroxide and a 120 J/cm<sup>2</sup> dose of 385 nm light containing 92% UV) reduced AIR-100 or ORL-200 viability below this threshold, providing support for the validity of this approach. No hazards were observed in EpiAirway for 425 nm light doses less than 160 J/cm<sup>2</sup> or in EpiOral for 425 nm light doses less than 120 J/cm<sup>2</sup> delivered at irradiance 50 mW/cm<sup>2</sup> (Table 2), suggesting conservatively that light doses less than 120 J/cm<sup>2</sup> are unlikely to cause cytotoxicity hazards in the oral cavity.

The second hazard assessed was the potential for acute oral cavity light dosing to disrupt the commensal bacteria of the oral microbiome. These organisms play an important role in oral health and disease, including inhibiting the growth of respiratory pathogens, and disruption of their growth could have potentially harmful consequences [27,28]. Both Gram-positive and Gram-negative strains were included in the panel assessed since each is known to respond differently to light. For example, Gram-positive organisms are thought to be generally more resilient due to their thicker peptidoglycan cell walls [29]. No bactericidal activity was observed against the Gram-positive model organism *S. mitis* at any 425 nm light dose tested (up to 192 J/cm<sup>2</sup>), and in the Gram-negative model organism *A. junii* no bactericidal activity was observed for 425 nm light doses less than or equal to 64 J/cm<sup>2</sup> at irradiance 50 mW/cm<sup>2</sup> (Table 2). Similar observations of light-induced bactericidal activity have been made previously by other groups; for example, it has been shown that 405 nm light doses of approximately 100 J/cm<sup>2</sup> or greater are required to significantly reduce growth of the pathogenic Gram-negative organism *Porphyromonas gingivalis* [30].

**Table 2**  
Non-hazardous 425 nm light dose ranges for the four hazards assessed.

Hazard	Model system	Light dose range tested	Maximum observed non-hazardous dose	Irradiance at maximum non-hazardous dose
Cytotoxicity	EpiAirway (AIR-100)	0–255 J/cm <sup>2</sup>	160 J/cm <sup>2</sup>	50 mW/cm <sup>2</sup>
Cytotoxicity	EpiOral (ORL-200)	0–120 J/cm <sup>2</sup>	120 J/cm <sup>2</sup>	50 mW/cm <sup>2</sup>
Commensal bactericidal effects	<i>S. mitis</i>	0–192 J/cm <sup>2</sup>	192 J/cm <sup>2</sup>	50 mW/cm <sup>2</sup>
Commensal bactericidal effects	<i>A. junii</i>	0–192 J/cm <sup>2</sup>	64 J/cm <sup>2</sup>	50 mW/cm <sup>2</sup>
Histopathological damage	Porcine esophagus sections	0–204 J/cm <sup>2</sup>	60 J/cm <sup>2</sup>	200 mW/cm <sup>2</sup>
Thermal damage	Oropharynx of intact porcine head	0–498 J/cm <sup>2</sup>	54 J/cm <sup>2</sup>	266 mW/cm <sup>2</sup>

Although this evaluation utilized a light source with a different peak wavelength and spectral distribution with significant UVA content than that used in the current study, the results provide additional support for bactericidal activity at and above 100 J/cm<sup>2</sup>. Because organisms that are killed by local high light doses would likely re-colonize the disrupted area from other sites in the oral cavity [31], *in vitro* testing is a conservative method of assessing the potential for microbiome disruption *in vivo*.

The cytotoxicity measurements in AIR-100 and ORL-200 provide an estimate of the light doses that are required to induce gross cell death, but they did not capture other pathological changes that could be induced through either photochemical or thermal mechanisms. Accordingly, the third hazard assessed was the potential for acute light doses to induce histopathological damage to the tissues of the oral cavity. A variety of characteristic histopathological changes have been observed in response to cutaneous burns [32], and verifying the absence of similar markers in response to oral cavity light delivery provides additional evidence that a light dose is of low hazard risk. In our study, histopathological damage was observed for 425 nm light doses of 120 J/cm<sup>2</sup> or greater (400 mW/cm<sup>2</sup> or greater for 5 min). Doses in this range resulted in a zone of increased hematoxylin staining in the lamina propria, basal cell vacuolization, changes to the smooth muscle layer, and nuclear streaming (a characteristic marker of thermal injury) in a majority of tissue sections. The presence of all of these markers suggests that doses of 120 J/cm<sup>2</sup> and greater are potentially hazardous and should be either be avoided in clinical testing, or, at a minimum, be delivered only under close monitoring. In contrast, no histopathological changes were observed for any light doses less than 120 J/cm<sup>2</sup>. Since the next highest dose tested was 60 J/cm<sup>2</sup>, we conservatively estimate the non-hazardous range for light-induced histopathological damage to be light doses less than or equal to 60 J/cm<sup>2</sup> delivered at irradiance 200 mW/cm<sup>2</sup> (Table 2).

The fourth hazard assessed is the potential for acute light doses to cause temperature increases that could induce thermal injury to the tissues of the oral cavity. Maximum allowable temperatures for medical devices are described in standards such as IEC 60601–1 [33], typically in terms of a maximum contact duration at a particular temperature. These standards are appropriate for evaluating devices that transfer heat to the body through conduction, for which the maximum device temperature provides a conservative estimate of the maximum temperature to which any subject tissue could increase. However, for devices that deliver thermal energy to tissues via radiation rather than conduction, this approach is insufficient. Alternative standard procedures have been developed by the medical imaging field, where exposure of human tissues to radiofrequency or microwave energies is common and so evaluation of radiation-induced thermal hazards is a standard practice. The foundational studies in this field administered a range of thermal treatments to a variety of human and porcine tissues and identified thresholds for damage in dozens of tissue types [23,34]. Measuring thermal damage thresholds in intact tissue accounts for factors that would not be captured in simpler model systems, such as the heat capacity of the intact tissue and heat dissipation via conduction to surrounding tissues. The oropharynx of the intact porcine head was considered a suitable choice due to the comparable dimensions and anatomical similarity of the oral cavity to that of humans. Because the measurements were performed with the tissue starting at ambient room temperature (to mitigate noise and temperature disturbances resulting from heating the tissue to physiological temperature), to compute the CEM<sub>43</sub> statistic we measured the temperature increase resulting from light treatment and added this to physiological temperature (37 °C) to estimate the temperatures that would be reached if the light doses were instead delivered *in vivo*. This approach assumes that the temperature increase resulting from light dosing is independent of the tissue's initial temperature. This assumption is supported by a first-order linear heat transfer model and is a reasonable approximation to make in this simplified model which does not account for more complex heat transfer

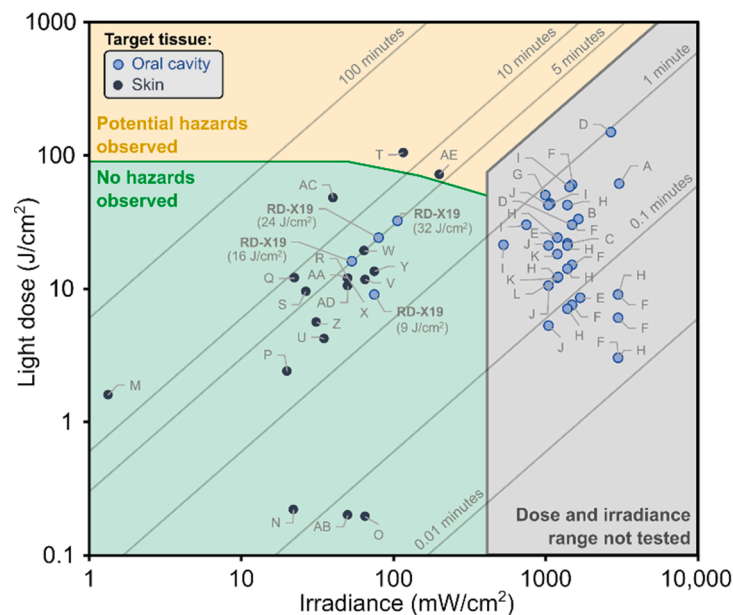
phenomena (such as convective cooling due to breathing, and evaporative heat transfer from secreted saliva) that could occur *in vivo*. Because these phenomena all tend to reduce tissue temperature (i.e., reduce thermal hazard risk), we considered this an appropriately conservative model with which to analyze thermal hazard test results.

Although thermal damage thresholds have been assessed in many different tissues [35], there has been limited work toward establishing thermal damage thresholds in the oral cavity. The most relevant available data are as follows: (1) thermal doses of 1–20 CEM<sub>43</sub> are typical thresholds for acute damage in tissues such as bone marrow, kidney, muscle, retina, and small intestine, (2) thermal doses of 20 CEM<sub>43</sub> resulted in “acute and significant damage” to porcine esophageal mucosa, and (3) thermal doses of >40 CEM<sub>43</sub> are needed to induce “significant and permanent” damage in skin [35,36]. Combining the results from the histopathological study presented here with previous work, CEM<sub>43</sub> <1 min was selected as a non-hazardous threshold in this pre-clinical assessment. The maximum observed non-hazardous light dose (one that resulted in CEM<sub>43</sub> < 1 min) was 54 J/cm<sup>2</sup>, delivered at irradiance 266 mW/cm<sup>2</sup> (Table 2).

In summary, our hazard assessments established a range of 425 nm light doses that are not cytotoxic to *ex vivo* well-differentiated human large airway or buccal epithelial models, are not bactericidal to commensal oral bacteria, do not induce histopathological damage in *ex vivo* porcine esophageal tissue, and do not cause a thermal hazard in the oral cavity as evaluated using the CEM<sub>43</sub> statistic. The tests and the corresponding non-hazardous light dose ranges identified are summarized in Table 2 and visualized schematically in Supplemental Fig. 3 in a plot of irradiance vs. dose. The green shaded region in Supplemental Fig. 3 indicates a range of doses and irradiances at which no hazards were observed at a lower dose and irradiance; notably, no hazards were observed for 425 nm light doses less than 63 J/cm<sup>2</sup> delivered at irradiance less than 200 mW/cm<sup>2</sup>. To demonstrate how this hazard assessment approach could be useful in a pre-clinical risk-benefit assessment, non-hazardous doses less than or equal to 60 J/cm<sup>2</sup> were delivered to artificial saliva samples containing SARS-CoV-2 and shown

to reduce SARS-CoV-2 viral titer in a dose dependent manner, with inactivation below the limit of detection of the assay occurring for a 425 nm light dose of 30 J/cm<sup>2</sup>, a dose which falls safely within the established non-hazardous range.

As a further extension of the work, the dose and irradiance of 31 representative FDA-cleared light dosing devices with wavelength similar to 425 nm were compiled and compared against the doses and irradiances of the hazard assessments conducted with 425 nm light in this study (Fig. 7). Devices operating across a range of wavelengths (370–515 nm) were selected for comparison to the 425 nm assessments because no FDA-cleared devices utilizing a single peak wavelength of 425 nm were identified. As a visual guide, a range of doses and irradiances was highlighted (in green; Fig. 7) at which a non-hazardous assessment was recorded at a higher dose and irradiance, and no potentially hazardous assessments were recorded at lower dose or irradiance. This highlighted region provides a conservative estimate of the doses and irradiances at which no hazards were observed in our study. Two existing FDA-cleared devices fall outside of this conservatively-defined non-hazardous dose and irradiance zone; these devices deliver 445–459 nm light to the skin for treatment of acne (device T) and psoriasis vulgaris (device AE). While these devices do fall in the potential hazard zone for 425 nm light, further work is needed to establish a relationship between wavelength and hazardous doses. Nevertheless, the existence of multiple FDA-cleared devices with doses and irradiances both inside and slightly outside of this non-hazardous zone supports that the preclinical hazard assessments are broadly consistent with existing work in the field and provides additional support for the safety of new devices operating with doses and irradiances inside the non-hazardous zone. As a specific example, RD-X19 [9], an oral cavity light-dosing investigational device, is under evaluation for the treatment of COVID-19 in clinical trials [11] at several doses and irradiances. All of the doses and irradiances being tested in the clinic fall within the non-hazardous region defined in this study (Fig. 7). Preclinical hazard assessments such as those described in this manuscript provide additional support for the safety and efficacy of new light-based medical



Label	Product	510(k) number	Wavelength
A	BluePhase PowerCure, dental curing light [Ivoclar Vivadent]	K190272	385 - 515 nm
B	LED Curing Light, dental curing light [EZGO Group]	K192009	370 - 550 nm
C	LED Curing Light, dental curing light [Foshan Dental Instrument Co]	K192233	430 - 490 nm
D	Cybird LED Curing Light [DXM Co., LTD]	K191221	405 nm
E	VALIANT Multispectral, dental curing light [Vista Apex]	K170101	400 - 500 nm
F	D1 LED Curing Light, dental curing light [DXM Co. LTD]	K121093	430 - 490 nm
G	Skylight, dental curing light [DMETEC]	K051571	440 - 490 nm
H	Sirius Max Dental Diode Curing Light [National Dental Inc]	K152936	430 - 490 nm
I	LC 2500 LED COMPACTA curing light [Lysta]	K992236	400 - 515 nm
J	LED Turbo-Pen [Apoza Enterprise Co. LTD]	K041303	440 - 490 nm
K	Bluephase Style 20i dental curing system [Ivoclar Vivadent, AG]	K163613	385 - 515 nm
L	Deml Ultra dental curing system [Kerr Dental]	K163064	450 - 470 nm
M	MMSphere, LED skin care device [MMSkincare]	K190443	465 nm
N	UI-200 Photon vibrating massage facial aesthetic device [LI-TEK]	K161434	405 - 425 nm
O	LED phototherapy device [LI-TEK]	K162098	412 - 418 nm
P	Pulsaderm, acne treatment device [Nutra Luxe]	K161941	410 - 420 nm
Q	Tanda Skincare System [Tanda]	K124042	408 - 420 nm
R	EP-300 Smart Photon Micro-current Device [LI-TEK]	K162652	405 - 425 nm
S	Acne Light Therapy Wand [Zuko]	K160691	438 - 446 nm
T	IlluMask, acne treatment device [LA Lumiere, LLC]	K123999	445 nm
U	LED Light Therapy Device [Uvbioteck]	K180900	407 - 427 nm
V	Quasar Calypso, anti-wrinkle device [Silver Bay LLC]	K111286	405 - 420 nm
W	"2 Face/ Face Evolution" [Heat In a Click LLC]	K171821	412 - 418 nm
X	Sonilase Blue, acne treatment device [BioRenew Labs]	K152889	410 - 420 nm
Y	Nutra Light Blue, acne treatment device [Nutra Luxe]	K132838	405 - 415 nm
Z	Clear Bi-Light, acne treatment device [Michael Todd, LP]	K153081	405 - 420 nm
AA	Elevare Sapphire, acne treatment device [Omm Imports]	K172555	410 - 420 nm
AB	Silk'n Blue, acne treatment device [Home Skinovations LTD]	K121435	400 - 430 nm
AC	OmniLux Clear-U, acne treatment device [Photo Therapeutics Inc]	K081307	410 - 420 nm
AD	LightStim, acne treatment [LightStim]	K142246	415 nm
AE	BlueControl, wearable psoriasis vulgaris treatment [Philips]	K171055	445-459 nm

Fig. 7. Review of doses and irradiances of a selection of FDA-cleared light-dosing devices. Dosing characteristics for selected FDA-cleared devices of similar wavelength that deliver light to the oral cavity (to cure dental composites) or skin (to treat a variety of conditions). For comparison, the green shaded region highlights a conservatively-defined range of doses and irradiances at which no potentially hazardous assay results were observed in this study, yellow highlights doses and irradiances that were potentially hazardous, and gray highlights doses and irradiances that were not evaluated in this study due to experimental limitations. As shown, no hazards were observed for 425 nm light doses less than 63 J/cm<sup>2</sup> delivered at irradiance less than 200 mW/cm<sup>2</sup>. In addition, dosing characteristics for RD-X19, an investigational device under development for the treatment of COVID-19 by applying 425 nm light to the oropharynx and surrounding tissues, are included for four doses tested clinically (9, 16, 24, and 32 J/cm<sup>2</sup>).

devices and help guide the initial selection of doses and treatment conditions.

Notably, all twelve of the FDA-cleared devices compiled in our review that deliver light to the oral cavity are intended for curing dental composites rather than delivering light to a tissue for therapeutic benefit (Fig. 7). In contrast, there exist devices that deliver light to the skin for a wide variety of therapeutic applications, in part because light doses can be delivered to the skin conveniently and non-invasively. Generally, devices that deliver light to the skin for therapeutic applications operate at lower irradiance ( $<200 \text{ mW/cm}^2$ ) than devices that deliver light to the oral cavity to cure dental composites ( $>500 \text{ mW/cm}^2$ ). This distinction highlights an opportunity to develop new devices to deliver light to the oral cavity at a lower irradiance for a range of potential therapeutic applications, mirroring the use of light-based therapies for skin, for which there are many predicate devices with a history of safe and effective use, though further work is needed to explore the differences in how skin *versus* oral tissues respond to light doses.

Although *in vitro* and *ex vivo* light hazard and *in vitro* viral inactivation assessments are an important complement to clinical evaluation, there are limitations to the ability of any preclinical study to model the response of human subjects to a candidate treatment. One important limitation of our study is that the *in vitro* assessments were performed under controlled conditions so they cannot directly account for human factors such as improper use of the light delivery device or anatomical variation between subjects. We sought to mitigate this limitation by establishing a comprehensive range of light doses that are non-hazardous and have demonstrated potential to inactivate SARS-CoV-2, to account for possible variability in the light dose delivered to different patients. A second limitation is that the antimicrobial and viral inactivation tests were performed under conditions that do not identically reflect the milieu of the oral cavity. We included a panel of representative organisms in the antimicrobial testing and completed the inactivation testing in multiple artificial salivas in response to these noted limitations. Finally, a third limitation is that none of the cytotoxicity, histopathological damage, or thermal damage assessments account for host response to the insult. For example, blood flow through and air flow over the tissues of the oral cavity are anticipated to reduce observed temperature increases in the *ex vivo* model employed here, correspondingly expanding the non-hazardous range of light doses. We sought to address this limitation by performing hazard assessments across a range of light doses, accounting for the possibility of host responses that could either increase or decrease the likelihood of observing a hazard at a given dose.

In spite of these limitations, we consider the approach presented in this work sufficient to establish that a non-hazardous dose of 425 nm light can serve as the basis for a light-based treatment for infections caused by SARS-CoV-2; however, we recognize that evaluation of potential hazards and predicted efficacy is an ongoing process, and any new candidate potential hazards or limitations to efficacy should be investigated through future preclinical *in vitro* and *ex vivo* studies. We also recognize that the ultimate evaluation of the prospective risks and offsetting benefits of any medical technology can only be completed through appropriate clinical trials and note that the 425 nm light doses delivered in both completed ( $16 \text{ J/cm}^2$ ) and ongoing ( $24 \text{ J/cm}^2$  and  $32 \text{ J/cm}^2$ ) trials have been informed by the work presented here [9,11,12].

## 5. Conclusions

Identifying a non-hazardous dose range through a combination of *in vitro* and *ex vivo* evaluations then evaluating potential efficacy at the same dose range *in vitro* is useful as a general framework for preclinical analysis of light-dosing therapies. Establishing and validating such a process is a critical step toward extending light-based therapies from the skin (where many safe and effective devices have been adopted for a variety of impactful applications) to other tissues of the body including those in the oral cavity. In this work, we combined preclinical hazard

assessments and SARS-CoV-2 inactivation efficacy to guide the development of a 425 nm light-based treatment for COVID-19. The process can be extended to other wavelengths, anatomical targets, and therapeutic applications to accelerate the development of novel photomedicine treatments.

## CRediT authorship contribution statement

**Max A. Stockslager:** Methodology, Formal analysis, Investigation, Writing – review & editing, Visualization. **Jacob F. Kocher:** Methodology, Formal analysis, Investigation, Visualization, Writing – review & editing. **Leslee Arwood:** Investigation. **Nathan Stasko:** Conceptualization, Methodology, Supervision, Investigation, Writing – review & editing. **Rebecca A. McDonald:** Investigation, Formal analysis, Visualization, Writing – review & editing. **Mark A. Tapsak:** Conceptualization, Methodology, Investigation, Writing – original draft, Writing – review & editing, Supervision. **David Emerson:** Conceptualization, Methodology, Writing – original draft, Writing – review & editing, Supervision.

## Declaration of Competing Interest

M.A.S., J.F.K., L.A., N.S., R.A.M., M.A.T., and D.E. conducted this work on behalf of EmitBio Inc. through their employment relationship with KNOWBIO, LLC., and may have ownership interest in one or both companies. J.F.K., N.S., R.A.M., M.A.T., and D.E. are inventors on patent applications/registrations owned by KNOWBIO, LLC.

## Acknowledgments

The authors wish to acknowledge Dr. Steve McClain (McClain Laboratories LLC) for performing histological evaluations; Dr. Andy Ruvo and Dr. Bill Van Alstine for providing comments on the manuscript; Madyson Chambers for performing commensal bacteria growth experiments; Adam Cockrell for contributions to the virus inactivation work; Michael Lay for contributing to figures; Steve Reich, Andrew Gaudet de Lestard, and Matt Womble for collaborating on the thermal measurements; and Ibrahim Henson for performing cytotoxicity experiments. This study was funded by EmitBio Inc. The following reagent was deposited by the Centers for Disease Control and Prevention and obtained through BEI Resources, NIAID, NIH: SARS-Related Coronavirus 2, Isolate USA-WA1/2020, NR-52281.

## Supplementary materials

Supplementary material associated with this article can be found, in the online version, at doi:10.1016/j.jdent.2022.104203.

## References

- [1] U. Khanna, S. Khandpur, What is new in narrow-band ultraviolet-B therapy for vitiligo? Indian Dermatol. Online J. 10 (2019) 234, <https://doi.org/10.4103/idoj.idoj.310.18>.
- [2] P.C. Göttsche, Niels Finsen's treatment for lupus vulgaris, J. R. Soc. Med. 104 (2011) 41–42, <https://doi.org/10.1258/jrsm.2010.10k066>.
- [3] G. Agati, F. Fusi, R. Pratesi, S. Pratesi, G.P. Donzelli, Colorful story of phototherapy for neonatal jaundice, in: S.B. Brown, B. Ehrenberg, J. Moan (Eds.), 1996: pp. 2–19. 10.1117/12.260751.
- [4] E.G. Richard, H. Hönigsmann, Phototherapy, psoriasis, and the age of biologics, Photodermatol. Photoimmunol. Photomed. 30 (2014) 3–7, <https://doi.org/10.1111/phpp.12088>.
- [5] M.R. Hamblin, Y.Y. Huang, Photobiomodulation in the Brain, Elsevier, 2019, <https://doi.org/10.1016/C2017-0-02758-1>.
- [6] N. Storm, L.G.A. McKay, S.N. Downs, R.I. Johnson, D. Birru, M. de Samber, W. Willaert, G. Cennini, A. Griffiths, Rapid and complete inactivation of SARS-CoV-2 by ultraviolet-C irradiation, Sci. Rep. 10 (2020), <https://doi.org/10.1038/s41598-020-79600-8>.
- [7] K. Imoto, N. Kobayashi, S. Katsumi, Y. Nishiwaki, W. Taka-Aki Iwamoto, A. Yamamoto, Y. Yamashina, T. Shirai, S. Miyagawa, Y. Dohi, S. Sugiura, T. Mori, The total amount of DNA damage determines ultraviolet-radiation-induced cytotoxicity after uniform or localized irradiation of human cells, 2002.

- [8] L. Zupin, R. Gratton, F. Fontana, L. Clemente, L. Pascolo, M. Ruscio, S. Crovella, Blue photobiomodulation LED therapy impacts SARS-CoV-2 by limiting its replication in Vero cells, *J. Biophotonics* 14 (2021), <https://doi.org/10.1002/jbio.202000496>.
- [9] N. Stasko, A.S. Cockrell, J.F. Kocher, I. Henson, D. Emerson, Y. Wang, J.R. Smith, N.H. Henderson, H. Wood, S.S. Bradrick, T. Jones, J. Santander, J.G. McNeil, A randomized, controlled, feasibility study of RD-X19 in subjects with mild-to-moderate COVID-19 in the outpatient setting, *Clin. Transl. Sci.* (2022), <https://doi.org/10.1111/cts.13249>.
- [10] N. Stasko, J.F. Kocher, A. Annas, I. Henson, T.S. Seitz, J.M. Miller, L. Arwood, R. C. Roberts, T.M. Womble, E.G. Keller, S. Emerson, M. Bergmann, A.N.Y. Sheesley, R.J. Strong, B.L. Hurst, D. Emerson, E.B. Tarbet, S.S. Bradrick, A.S. Cockrell, Visible blue light inhibits infection and replication of SARS-CoV-2 at doses that are well-tolerated by human respiratory tissue, *Sci. Rep.* 11 (2021), <https://doi.org/10.1038/s41598-021-99917-2>.
- [11] EmitBio Inc., NCT04966013: evaluation of the RD-X19 treatment device in individuals with mild to moderate COVID-19, *ClinicalTrials.gov.* (2022).
- [12] EmitBio Inc., NCT04662671: phase I/II randomized, dose escalation study to evaluate the safety and antiviral activity of the RD-X19 device in SARS-CoV-2 infected individuals with uncomplicated COVID-19, (2021).
- [13] J. Kocher, L. Arwood, R.C. Roberts, I. Henson, A. Annas, N. Stasko, M. Leslie Fulcher, M. Brotton, S.H. Randell, Visible blue light inactivates SARS-CoV-2 variants and inhibits delta replication in 1 differentiated human airway epithelia 2, *bioRxiv.* (2022). 10.1101/2022.01.25.477616.
- [14] International Organization for Standardization, ANSI/AAMI/ISO 10991-1:2009/(R)2013 biological evaluation of medical devices – part 1: evaluation and testing within a risk management process, 2009.
- [15] P. Kumar, A. Nagarajan, P.D. Uchil, Analysis of cell viability by the MTT assay, *Cold Spring Harb. Protoc.* 2018 (2018), <https://doi.org/10.1101/pdb.prot095505>.
- [16] G.R. Jackson, A.G. Maione, M. Klausner, P.J. Hayden, Prevalidation of an acute inhalation toxicity test using the EpiAirway *in vitro* human airway model, *Appl. In Vitro Toxicol.* 4 (2018) 149–158, <https://doi.org/10.1089/avt.2018.0004>.
- [17] Student, The probable error of a mean, *Biometrika* 6 (1908) 1–25.
- [18] E.M. Bik, C.D. Long, G.C. Armitage, P. Loomer, J. Emerson, E.F. Mongodin, K. E. Nelson, S.R. Gill, C.M. Fraser-Liggett, D.A. Relman, Bacterial diversity in the oral cavity of 10 healthy individuals, *ISME J.* 4 (2010) 962–974, <https://doi.org/10.1038/ismej.2010.30>.
- [19] W. Crielaard, E. Zaura, A.A. Schuller, S.M. Huse, R.C. Montijn, B.J.F. Keijsers, Exploring the oral microbiota of children at various developmental stages of their dentition in the relation to their oral health, *BMC Med. Genom.* 4 (2011), <https://doi.org/10.1186/1755-8794-4-22>.
- [20] M. Costalonga, M.C. Herzberg, The oral microbiome and the immunobiology of periodontal disease and caries, *Immunol. Lett.* 162 (2014) 22–38, <https://doi.org/10.1016/j.imlet.2014.08.017>.
- [21] G.M. Gray, H.J. Yardley, Lipid compositions of cells isolated from pig, human, and rat epidermis, *J. Lipid Res.* 16 (1975) 434–440, [https://doi.org/10.1016/S0022-2275\(20\)34493-X](https://doi.org/10.1016/S0022-2275(20)34493-X).
- [22] R.C. Wester, J. Melendres, L. Sedik, H. Maibach, J.E. Riviere, Percutaneous absorption of salicylic acid, theophylline, 2,4-dimethylamine, diethyl hexyl phthalic acid, and p-aminobenzoic acid in the isolated perfused porcine skin flap compared to man *in vivo*, *Toxicol. Appl. Pharmacol.* 151 (1998) 159–165, <https://doi.org/10.1006/taap.1998.8434>.
- [23] P.S. Yarmolenko, E.J. Moon, C. Landon, A. Manzoor, D.W. Hochman, B.L. Viglianti, M.W. Dewhirst, Thresholds for thermal damage to normal tissues: an update, *Int. J. Hyperther.* 27 (2011) 320–343, <https://doi.org/10.3109/02656736.2010.534527>.
- [24] G.C. van Rhoon, T. Samaras, P.S. Yarmolenko, M.W. Dewhirst, E. Neufeld, N. Kuster, CEM43°C thermal dose thresholds: a potential guide for magnetic resonance radiofrequency exposure levels? *Eur. Radiol.* 23 (2013) 2215–2227, <https://doi.org/10.1007/s00330-013-2825-y>.
- [25] S.B. Field, C.C. Morris, The relationship between heating time and temperature: relevance to clinical hyperthermia, *Radiother. Oncol.* 1 (1983) 17–186.
- [26] S.A. Sapareto, W.C. Dewey, Thermal dose determination in cancer therapy, *Int. J. Radiat. Oncol. Biol. Phys.* 10 (1984) 787–800, [https://doi.org/10.1016/0360-3016\(84\)90379-1](https://doi.org/10.1016/0360-3016(84)90379-1).
- [27] R. Khan, F.C. Petersen, S. Shekhar, Commensal bacteria: an emerging player in defense against respiratory pathogens, *Front. Immunol.* 10 (2019), <https://doi.org/10.3389/fimmu.2019.01203>.
- [28] J.L. Baker, B. Bor, M. Agnello, W. Shi, X. He, Ecology of the oral microbiome: beyond bacteria, *Trends Microbiol.* 25 (2017) 362–374, <https://doi.org/10.1016/j.tim.2016.12.012>.
- [29] P.D. Williams, S.L. Eichstadt, T.A. Kokjohn, E.L. Martin, Effects of ultraviolet radiation on the Gram-positive marine bacterium *Microbacterium maritimum*, *Curr. Microbiol.* 55 (2007) 1–7, <https://doi.org/10.1007/s00284-006-0349-2>.
- [30] C.K. Hope, J.A. Hindley, Z. Khan, E. de Josselin de Jong, S.M. Higham, Lethal photosensitization of *Porphyromonas gingivalis* by their endogenous porphyrins under anaerobic conditions: an *in vitro* study, *Photodiagn. Photodyn. Ther.* 10 (2013) 677–682, <https://doi.org/10.1016/j.pdpdt.2013.08.006>.
- [31] J.L. Mark Welch, S.T. Ramírez-Puebla, G.G. Borisy, Oral microbiome geography: micron-scale habitat and niche, *Cell Host Microbe* 28 (2020) 160–168, <https://doi.org/10.1016/j.chom.2020.07.009>.
- [32] D.A. Hirth, A.J. Singer, R.A.F. Clark, S.A. McClain, Histopathologic staining of low temperature cutaneous burns: comparing biomarkers of epithelial and vascular injury reveals utility of HMGB1 and hematoxylin phloxine saffron, *Wound Repair Regen.* 20 (2012) 918–927, <https://doi.org/10.1111/j.1524-475X.2012.00847.x>.
- [33] International Electrotechnical Commission, IEC 60601-1 Medical electrical equipment – part 1: general requirements for basic safety and essential performance, 2012.
- [34] M. Dewhirst, B.L. Viglianti, M. Lora-Michiels, P.J. Hoopes, M.A. Hanson, Thermal dose requirement for tissue effect: experimental and clinical findings. *Thermal Treatment of Tissue: Energy Delivery and Assessment II*, SPIE, 2003, p. 37, <https://doi.org/10.1117/12.476637>.
- [35] P.S. Yarmolenko, E.J. Moon, C. Landon, A. Manzoor, D.W. Hochman, B.L. Viglianti, M.W. Dewhirst, Thresholds for thermal damage to normal tissues: an update, *Int. J. Hyperther.* 27 (2011) 320–343, <https://doi.org/10.3109/02656736.2010.534527>.
- [36] G.C. van Rhoon, T. Samaras, P.S. Yarmolenko, M.W. Dewhirst, E. Neufeld, N. Kuster, CEM43°C thermal dose thresholds: a potential guide for magnetic resonance radiofrequency exposure levels? *Eur. Radiol.* 23 (2013) 2215–2227, <https://doi.org/10.1007/s00330-013-2825-y>.